AEROBRAKING PERICENTRE CONTROL STRATEGIES

Filippo Cichocki[(1)], Mariano Sanchez[(1)], Sebastien Clerc[(2)], Thomas Voirin[(3)]

[(1)] Deimos Space, Ronda de Poniente 19, Tres Cantos 28760, Madrid, Spain
filippo.cichocki@deimos-space.com, mariano.sanchez@deimos-space.com
[(2)] Thales Alenia Space France. sebastien.clerc@thalesaleniaspace.com
[(3)] European Space Agency. thomas.voirin@esa.int

ABSTRACT

In the context of space missions with a demanding payload mass about celestial bodies with atmosphere, aerobraking emerges as an enabling technology.
This technique allows transforming a highly elliptical insertion orbit into a nearly circular, low-altitude orbit by a sequence of free atmospheric passes. As the S/C passes through the outer layers of the atmosphere, the orbit energy is reduced by the aerodynamic forces acting on the solar array. The consequent panel temperature rise has to be fully controlled, thus requiring the definition of aerobraking corridors that ensure structural safety at a given confidence level.
Although the most efficient way to define such corridor is to use the **solar array temperature** as the direct control variable, such approach presents several drawbacks such as the difficulty of predicting it or the complex issue of number and location of sensors.
The easier predictability of surrogate variables like peak heat flux, peak dynamic pressure and heat load per pass makes them more suitable for corridor definition. In this paper, two approaches based on one and two surrogate variables will be described.
In order to discuss these approaches, comparative performance assessments will be shown for these strategies when applied to mission scenarios around Mars, Venus and Titan.

1. INTRODUCTION

Nowadays more and more space exploration missions are demanding to put a significantly big payload in orbit around a planet. Typical goals are those of observing the planet, its atmosphere, some of its satellites from a close distance or to provide a relay orbiter for future surface exploration landers.

Injection of the S/C into the low altitude orbit required for this purpose was generally achieved in the past by applying a large chemical burn at the arrival hyperbola pericentre. The deltaV cost of this type of injection grows as the arrival infinite velocity increases and as the target orbit size shrinks. Therefore, the high cost of such injections generally limited either the final mass ratio or the minimum altitude about the celestial body.

However, if the planet presents an atmosphere, aerobraking can provides a great improvement of the final mass ratio. With this technique, the orbit energy is reduced through a series of successive atmospheric passes rather than by a large chemical burn. On the other hand, however, aerobraking is **technically more complicated, longer and operationally more demanding**. In fact, in order to follow a given baseline timeline of apocentre altitude reduction while not endangering the S/C structures, a control corridor must be defined and fulfilled throughout the aerobraking. The purpose of this paper is to provide a feasible definition of this corridor and to present some relevant examples of application for different scenarios.

Aerobraking was firstly demonstrated technically by NASA in 1993 with the Magellan mission about Venus, which reached a very low altitude orbit by successive atmospheric passes in the Venus's atmosphere. Later on, aerobraking has been used as an enabling technology for various NASA missions targeting low altitude orbits around Mars, like the Mars Global Surveyor, the Mars Odyssey and the Mars Reconnaissance Orbiter.

Various future missions are being planned nowadays that envisage aerobraking as an enabling technology. The NASA/ESA mission "Exomars", for example, is featuring an aerobraking strategy in its current baseline mission scenario in order to insert the S/C about Mars in 2016/2017. The objective is that of studying the Mars atmosphere and guaranteeing a relay orbit for communication with two surface exploration landers which are expected to arrive two years later.

The ESA Mars Sample Return Mission is another mission to Mars envisaged for launch in the first half of the 2020s. This mission aims at collecting Mars surface rocks and dust samples and bringing them back to Earth. Upon arrival to Mars, an orbiter will separate from a descent module and reach a final relay orbit through an aerobraking phase. Once the Mars sample has been released into orbit by a dedicated Mars Ascent Vehicle, the orbiter will dock with it and start the long journey back to Earth.

Titan is also drawing interest in the context of aerobraking missions. The NASA/ESA TSSM mission, envisaged for the decade 2020-2030, features an aerobraking phase of the S/C about the Saturn's satellite, during which, detailed analysis of the atmosphere should be carried out.

2. AEROBRAKING CORRIDOR CONTROL

The aerobraking corridor characterizes the Main Phase, which is the longest of the three main phases building an aerobraking strategy. Complete information about these phases can be found in [1]. Here we provide only a brief description:

- Walk-In: Gradual lowering of the pericentre altitude of an initial highly elliptical orbit. It allows reaching the operational aerobraking working conditions in the safest way and permits to tune the predictive atmosphere model to the actual atmospheric conditions
- Main Phase: it is the phase providing most of the apocentre altitude reduction and requiring the most demanding orbit control. This is achieved by forcing the S/C to stay within an aerobraking control corridor
- Walk-Out: final phase achieving the desired final orbit, while keeping the orbit lifetime above a minimum allowed value. Lifetime is the time required by the apocentre altitude to get below a threshold value if no pericentre raising manoeuvres were performed

The control corridor permits to accomplish the apocentre altitude reduction within a given maximum time while keeping the S/C structures safe. The time requirement is achieved by defining a "corridor lower boundary", while the safety requirement is satisfied with the definition of a "corridor upper boundary".

Traditionally, the aerobraking corridor has been defined in terms of easily predictable control variables, such as the peak dynamic pressure and the peak heat flux at pericentre. The former, characterizing the corridor definition of the MGS mission ([2] and [3]) is computed as in Equation (1), where ρ is the atmospheric density and V_{atm} is the velocity of the S/C relative to the wind:

$$p_{dyn\ peak} = \max\left(\frac{1}{2}\cdot\rho\cdot V_{atm}{}^{2}\right)_{drag\ pass} \qquad (1)$$

The peak heat flux, on the other hand, is proportional to the cube of V_{atm}, as shown in equation (2):

$$\Phi_{peak} = \max\left(\frac{1}{2}\cdot\rho\cdot V_{atm}{}^{3}\right)_{drag\ pass} \qquad (2)$$

In order to make the S/C comply with a corridor, small chemical burns are periodically applied at apocentre to control the pericentre altitude evolution. Each burn is computed so as to guarantee that the control variable fulfils as much as possible the corridor at least up to the following burn decision epoch (we refer to the time interval between successive manoeuvres decisions as to the "**control interval**").

Figure 1 shows three examples of the effect of an aerobraking manoeuvre (ABM). First of all, the evolution of the control variable throughout one control interval is predicted (red circles in Figure 1). If, for any drag pass, the control variable occurs to be outside of the corridor, then an ABM is computed and applied at the first apocentre to bring the highest predicted control variable (representing the worst drag pass) to the upper corridor boundary (blue circles).

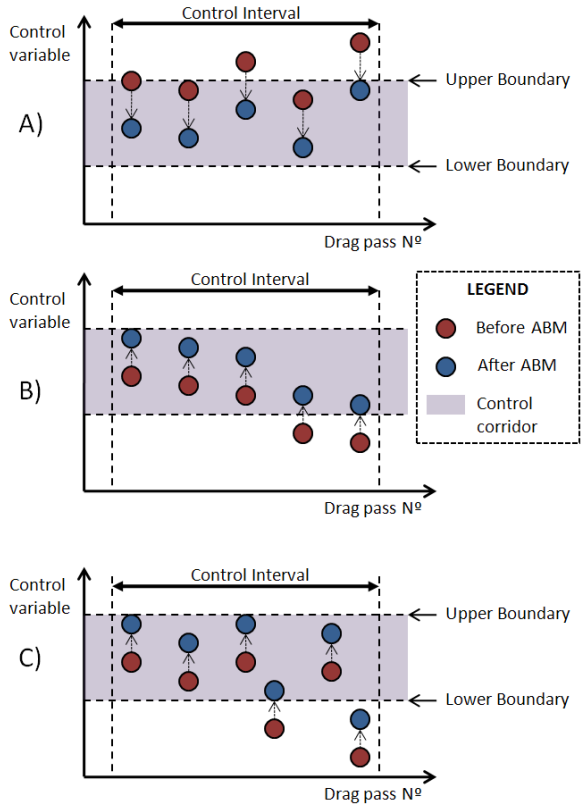

Figure 1: ABM effect on control variable evolution

In case A), an upper boundary violation is detected and the ABM raises the pericentre altitudes by the minimum amount necessary to comply with the

corridor (the control variable evolution shifts downwards).

In case B), a lower boundary violation is detected and the ABM lowers the pericentre as much as permitted by the corridor (i.e. until the worst drag pass control variable has reached the upper boundary). In this way, the duration of the Main Phase is minimized.

There is one particular case, depicted in case C), in which the ABM is not enough to force all control variables to stay within the corridor. This occurs when the control variable presents a natural dispersion bigger than the corridor width.

The corridor control approach described above is the one yielding the lowest aerobraking duration while controlling the maximum manoeuvres frequency (ABMs are computed, if necessary, every control interval and hence their frequency is fully controlled). In the next chapter, we shall provide a feasible approach for the definition of the control corridor.

3. DEFINING A CONTROL CORRIDOR

As we have already pointed out in the previous chapter, the aerobraking corridor consists of two boundaries. The lower boundary must ensure that a minimum drag deltaV be achieved for each pass (or a minimum period reduction). On the other hand, the upper boundary must prevent any structural damage due to excessive thermal or mechanical stresses.

The driving constraint for the majority of the aerobraking missions is the thermal stress. In fact, the most critical component is the solar array, the surface of which is oriented at 90º with respect to the wind velocity during the drag pass. The heat generated by the impact of free molecules results into a solar array temperature rise that has to be controlled throughout the Main Phase.

Therefore, it seems to be very efficient to define the aerobraking corridor with the solar array peak temperature as the direct control variable. Such approach would feature a constant upper corridor boundary set at the maximum allowed solar array temperature. However, there are several drawbacks for this approach.

First of all, the computation of the ABM necessary to comply with the control corridor requires the non-trivial capability of predicting accurately the solar panel temperature up to several orbits ahead (refer to Figure 1), which means to have a very accurate thermal model of the S/C. Furthermore, during mission operations, in order to verify that the corridor is not being violated, it would be necessary to place some temperature sensors at specific appropriate locations of the solar panel, which is again another complex task.

For the above reasons, it has been traditionally preferred to use surrogate variables like peak heat flux or dynamic pressure to define the aerobraking corridor. Both the peak heat flux and dynamic pressure are very easy to compute (equations (1) and (2)) since they depend only on the orbit geometry and atmospheric density. Moreover, peak dynamic pressure and heat flux are closely related to the drag DeltaV per pass (the peak dynamic pressure is almost proportional to it) and therefore, the corridor lower boundary can be expressed as an elementary function.

Although the definition of the lower boundary is fairly simple (a fixed value of peak dynamic pressure for example), the major drawback of the surrogate variables is the fact that a given peak value of heat flux or dynamic pressure does not correspond always to a given peak solar array temperature. In fact, the temperature rise does not depend solely on the peak value of the heating rate (or heat flux), but also on the duration of the drag pass. Such duration is a function of the orbital geometry because, as the orbit shrinks and the eccentricity lowers, the fraction of orbit spent inside the atmosphere gets longer. For Mars missions, the drag pass duration may change from an initial 5 minutes to more than 20 minutes towards the end of the aerobraking.

Figure 2 shows how different two temperature profiles might look like even when presenting the same peak heat flux. The dotted curves refer to a short duration pass, while the continuous curves to a long duration pass. The temperature always lags behind the heat flux because of the finite thermal inertia of the solar array.

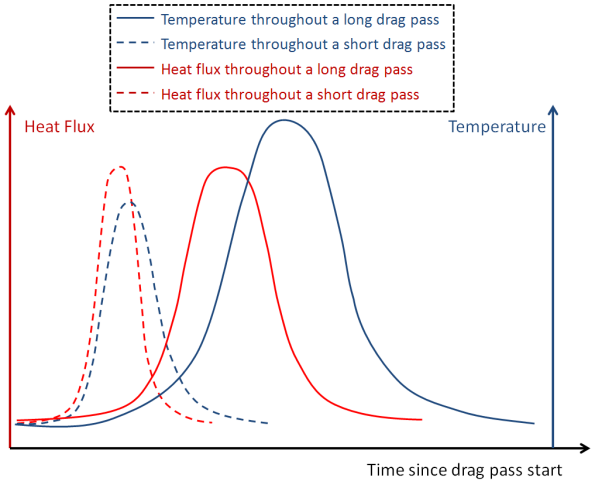

Figure 2: Evolution of temperature for two orbits presenting same peak heat flux and different duration

This means that the solar panel is never in thermal equilibrium between the absorbed heat (from drag

friction) and the heat emission (from temperature). For this reason, the peak temperature does not depend only on the peak heat flux but also on the pass duration, thus reaching higher values for longer passes.

The corridor upper boundary definition must then take into account the orbital geometry or the integrated heat flux:

$$T_{peak} = T_{peak}\left(\Phi_{peak}, \Delta Q\right) \quad (3a)$$

$$T_{peak} = T_{peak}\left(\Phi_{peak}, orbit\ geometry\right) \quad (3b)$$

In equation (3a), the integrated heat flux, or heat load, is defined as:

$$\Delta Q = \int_{Atmospheric\ pass} \Phi\, dt \quad (4)$$

Equations (3a) and (3b) are not completely equivalent, as it will later be shown. However, starting from these two equations, it is possible to derive two feasible corridor upper boundary definitions:

- **1-D Corridor**: by equating the left hand side of Equation (3b) to the maximum allowable temperature T_{max} and inverting the equation, it is possible to express the upper boundary flux as:

$$\Phi_{upper\ boundary} = f(T_{\max}, geometry) \quad (5)$$

  The geometry dependence can be obtained by expressing the maximum allowable heat flux as a function of the apocentre altitude, because the pericentre altitude stays practically unchanged. Each drag pass must then present a heat flux lower than the upper boundary value corresponding to the current apocentre altitude. The approach is clearly applicable even when using the peak dynamic pressure as the control variable (just substitute Φ with p_{dyn} in the previous equations)

- **2-D Corridor**: by equating the right hand side of equation (3a) to the maximum allowed temperature T_{max}, it is possible do define a 2-D curve in the heat flux/ heat load plane. Each pericentre pass is represented by one point in such plane and must be forced to remain below such upper boundary curve:

$$T_{peak}(\Phi_{peak}, \Delta Q) = T_{\max} \quad (6)$$

For both approaches, the maximum allowable temperature is determined as the maximum temperature that the solar array can withstand, divided by a safety margin accounting for atmosphere density uncertainties. Such margin should generally be tested with aerobraking Montecarlo simulations with a perturbed atmosphere to see if the corridor assumption is conservative enough.

There are some differences between the 1-D and 2-D corridor approaches. If, on one hand, the former is simpler since it takes into account only one control variable, the latter presents the advantage of featuring a fixed corridor throughout the aerobraking. In addition, the 2-D approach is slightly more efficient as it will be demonstrated below.

Refer to Figure 4, showing two atmospheric passes with the same geometry, same peak heat flux but with a different value of the atmosphere scale height (characteristic length over which the density changes by a factor of *e*). Red lines refer to a scale height of 8.6 km and the blue lines to a scale height of 7 km. This difference might arise because of a different drag pass longitude. Although the 1-D corridor upper boundary would provide the same heat flux in both cases, the peak temperature would be higher for the case featuring a higher scale height, as shown in Figure 4. This means that equation (3b) does not take into account the density scale height influence. On the other hand, the 2-D corridor definition is nearly independent of the assumed atmospheric scale height, because the latter affects both the heat load and the peak temperature values. Such non-optimality of the 1-D corridor approach, however, is quite small, since temperature differences due to the different scale heights only amount to a few degrees Celsius.

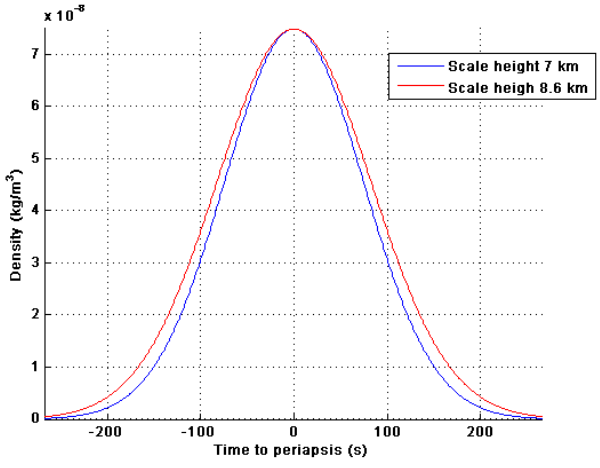

Figure 3: Two drag pass profiles with same peak density (and heat flux) and different scale heights

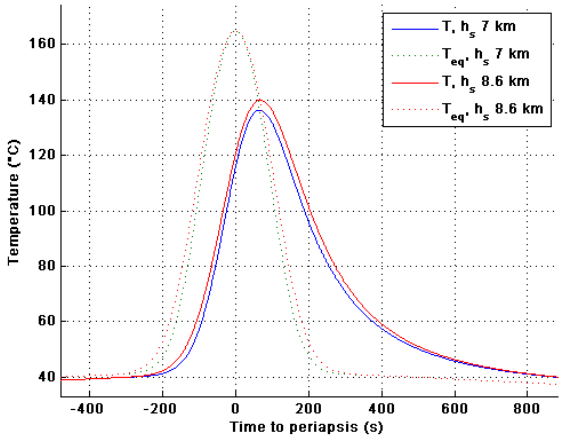

Figure 4: Dependence of the peak panel temperature on the atmospheric scale height

To summarize, Table 1 shows the pros and cons of the corridor approaches described in this paragraph. The solar array temperature approach is clearly the most efficient since it controls the real constraint variable but it presents several drawbacks for what concerns its implementation. The 1-D and 2-D corridor approaches with surrogate variables differ from each other for a slightly higher efficiency of the latter. Nevertheless, the 1-D corridor approach is simpler and preferable when the upper constraint of the corridor is not related to a peak solar array temperature but rather to other factors or during early stages of a mission design process when detailed geometry and characteristic of the S/C are not available yet (see Titan's aerobraking mission simulation).

Table 1: Comparison of the corridor control options

	PROs	CONs
Solar array temperature	• Direct derivation of upper corridor boundary • Highest efficiency	• Prediction of temperature • Temperature sensors positioning • No simple definition of lower boundary
1-D Heat Flux or Pdyn corridor	• Easy to implement • Adaptable to any desirable timeline	• Non-optimality
2-D heat flux - heat load corridor	• Fixed corridor • High efficiency	• Higher complexity for ABM decisions

4. SIMPLIFIED THERMAL MODEL

As described in the previous section, the Solar Array temperature is a key input for the definition of the aerobraking corridor. A simplified model is required to predict the solar array temperature and its dependence on the flight parameters. A balance has to be found between simplifying assumptions (requiring worst case assumptions or margins) and complexity.

More precisely, the following simplifications have been made:

- Single node thermal model: the thermal gradient between the front and back sides of the array (typically 10 K) is neglected
- Solar Array thermally decoupled from the spacecraft body (conductive and radiative exchanges are neglected)
- Uniform convective heat transfer coefficient equal to 1: this is a quite conservative assumption

Simplifications have been also made to account for environmental fluxes. Note that neglecting totally the environmental flux is not justifiable, especially because it would yield a null equilibrium temperature outside the atmosphere. The following description is considered:

- The solar flux at the considered heliocentric distance is taken into account during the whole aerobraking pass, at normal incidence. This is obviously a worst case conservative assumption
- The planetary infrared flux is considered, assuming that the solar array is perpendicular to the radius vector from the planet centre
- The planetary albedo is also taken into account, assuming again a normal incidence.

More precisely, the planetary flux (Infrared + albedo) is computed as given in Equation (7):

$$\Phi_{Planet} = \Phi_{Sun}\left(C_a + C_t\right)\left(\frac{R}{R+h}\right)^2, \qquad (7)$$

where Φ_{Sun} is the incoming solar flux, C_a and C_t are respectively the planet albedo and thermal infrared coefficients, R is the planet radius and h the spacecraft altitude.

Once these simplifications have been made, it is possible to compute the evolution of the Solar Array temperature during an aerobraking pass, as a result of the balance between the incoming convective flux and environmental fluxes and the outgoing radiative flux toward space, as given in Equation (8):

$$mC_p\dot{T} = \Phi_{conv} + (\alpha_1 + \alpha_2)\Phi_{Planet} + \ldots \\ \max(\alpha_1, \alpha_2)\Phi_{Sun} - \sigma(\varepsilon_1 + \varepsilon_2)T^4, \quad (8)$$

where mC_p is the thermal inertia of the solar panel, $\alpha_{1,2}$ and $\varepsilon_{1,2}$ are the thermal absorptance and emissivity coefficients of the solar panel surfaces (front and back surfaces), and σ is the Stefan-Boltzmann constant. Note that the solar flux is applied to the most absorbing surface (worst case) whereas the infrared, albedo and outgoing radiative fluxes are applied to both surfaces. Typical values for these parameters are listed in Table 3.

The initial temperature at the beginning of the pass required for the integration of the thermal dynamics is the equilibrium temperature under environmental fluxes only (negligible convective flux), as given in Equation (9):

$$T_0 = \left[\frac{\max(\alpha_1, \alpha_2)\Phi_{Sun} + (\alpha_1 + \alpha_2)\Phi_{Planet}}{\sigma(\varepsilon_1 + \varepsilon_2)} \right]^{1/4} \quad (9)$$

5. AEROBRAKING CORRIDOR ALGORITHM

The thermal model described in the previous section is used to predict the maximum temperature of the solar array during the aerobraking pass. Note that because of the thermal inertia, the maximum temperature is reached after the pericentre (peak of the convective heat flux). While an exact aerobraking altitude and heat flux profile could be used at this point, a first-order approximation of the trajectory around the pericentre allows to speed-up the simulation time and remains compatible with the required accuracy for the definition of the aerobraking corridor. Similarly, a simple scale-height model is sufficient to describe the atmospheric density.

As explained in section 3, the relevant parameters for the prediction of the peak temperature are the peak heat flux and the heat load. However one needs to use other parameters (pericentre, apocentre and atmosphere model parameters) to compute the temperature evolution. It can be shown that a modification of these parameters leading to the same peak heat flux and heat load yields the same peak temperature.

The model described above allows to predict, for given apocentre and pericentre altitudes and atmosphere parameters, the peak solar array temperature. The block is used within an iterative scheme in order to define the aerobraking corridor.

The procedure is as follows:

1. For each value of the apocentre altitude in the aerobraking range,
2. Find the pericentre altitude such that the maximum allowable Solar Array temperature T_{max} is reached
3. Record the resulting values of the peak heat flux and heat load.

Step 2 is itself the result of an inner iteration (a root finder featuring a simple dichotomy algorithm). The overall procedure is depicted in Figure 5. Here H_a and H_p are respectively the pericentre and apocentre altitudes, whereas H(t) and V(t) are the keplerian profiles of altitude and inertial velocity. At the beginning of the loop, a pericentre altitude attempts is computed as the mean value of a pericentre altitude range [$H_{p\ min}$, $H_{p\ max}$] which is continuously adjusted during the root finder convergence.

A similar approach can be used to define the lower limit of the corridor (minimum dynamic pressure). In this case, the thermal model is not required. The dichotomy algorithm is still used for convenience at step 2, although the simpler dependence of the dynamic pressure with respect to the pericentre altitude (exponential dependence at first order) allows, in principle, a more efficient implementation. The algorithm for determining the lower boundary of the corridor is depicted in Figure 6.

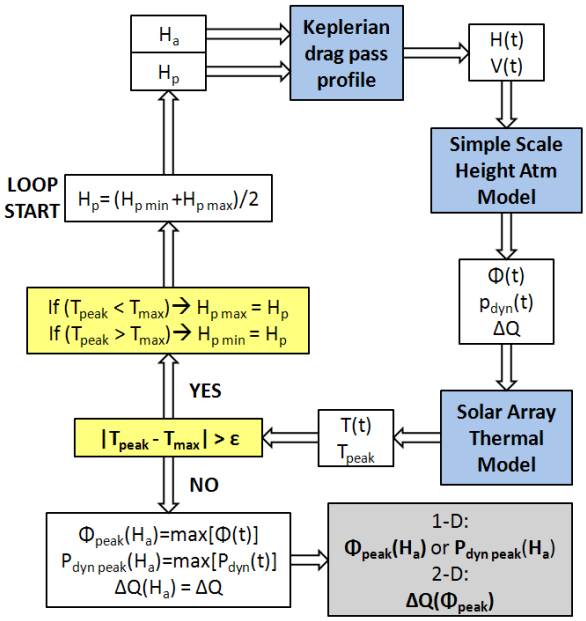

Figure 5: Aerobraking corridor upper limit definition algorithm

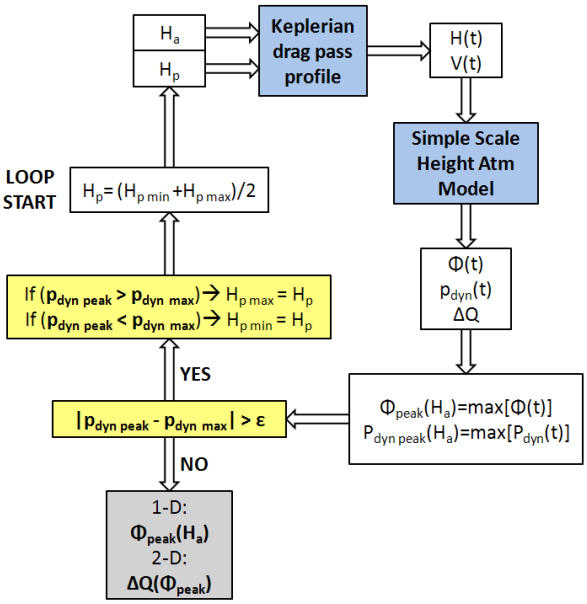

Figure 6: Aerobraking corridor lower limit definition algorithm

6. AEROBRAKING SIMULATION ON MARS

The mission about Mars selected for this paper is the **Mars Sample Return Orbiter mission** (MSRO), scheduled by ESA for launch in the first half of 2020s. Such mission features an aerobraking phase for the acquisition of the orbiter relay orbit. Table 2 summarises the aerobraking parameters used for the current simulation.

The initial orbital period in approximately ½ Sol (nearly 12 hours) and the initial inclination is 45°. The Walk-In phase consists of a gradual lowering of the pericentre altitude (through 8 successive burns) starting from an initial pass of 150 km of altitude. During the Main Phase, ABMs are separated by at least 2 days, (control interval duration). Main Phase exit condition is the remaining S/C lifetime approaching 4 days whereas the Walk-Out terminates when the apocentre has lowered to 600 km with a final circularisation burn.

Table 2: Parameters of the aerobraking simulation

Aerobraking parameters	Value
Initial orbital period (Sol)	0.5
Initial inclination (deg)	45.0
Initial Walk-In pericentre altitude (km)	150.0
Number of Walk-In ABMs	8
Control interval duration (days)	2.0
Minimum allowed lifetime (days)	4.0
Reference altitude for lifetime computation (km)	350.0
Final circular orbit altitude (km)	600.0
S/C ballistic coefficient (kg/m^2)	56.5

Orbit propagation takes into account the following:

- Non-spherical gravity of degree and order 5
- Sun gravity perturbation.
- Atmospheric drag modelled with EMCD V4.3 Mars atmosphere model, Warm Scenario (6)

Both the 1-D and 2-D control corridor cases have been simulated. In order to obtain the corridors, a parametric analysis with varying atmosphere scale heights has been performed (respectively 7, 8 and 9 km).

The other parameters used to define the corridor are listed in Table 3. The **upper boundary** has been computed with a **maximum allowable temperature of 95°C**, whereas the **lower boundary** with a **peak dynamic pressure** of **0.15 N/m^2**. The maximum allowable temperature is lower than the highest temperature that the solar array can withstand (150°C). This is typical for Mars missions, because the atmosphere uncertainty requires that a big safety margin be assumed.

Table 3: Solar array and environmental parameters for Mars AB corridor definition

Parameter	Value
Mars Bond Albedo	0.29
Solar array specific heat per unit surface (J/(K·m^2))	2241.0
Absorption coefficient of solar array back side coating (carbon fiber), α_2	0.9
Absorption coefficient of solar cells, α_1	0.86
Emissivity coefficient of array back side ε_2 coating	0.79
Emissivity coefficient of solar cells, ε_1	0.87
Solar flux (W/m^2)	600.0
Maximum allowable array temperature (°C)	95°C
Minimum peak dynamic pressure (N/m^2)	0.15

Figure 7 shows the 1-D upper boundary dependence on the scale height. If the scale height is higher, the expected peak solar array temperature is higher for a given peak heat flux. Therefore, the upper boundary lowers by approximately 100 W/m^2 when the scale height rises from 7 km up to 9 km.

The lower boundary, on the other hand, remains unaffected. In fact, at a given apocentre altitude, the peak dynamic pressure is a function of the only peak heat flux, with no dependence on scale height.

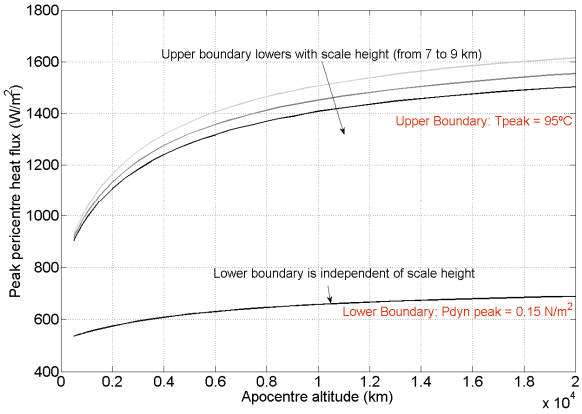

Figure 7: 1-D corridor sensibility to scale height assumption

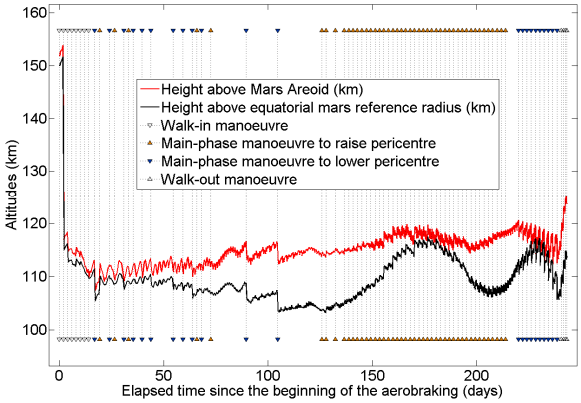

Figure 9: 2-D Corridor simulation, pericentre altitude evolution and ABMs effect

Figure 8 shows the dependence of the 2-D corridor on the scale height assumption. As expected, the upper boundary is almost independent of it. The lower boundary curve, on the other hand, tends to rise with the scale height because, at a given peak heat flux (and hence peak dynamic pressure) the heat load grows with the scale height (density decreases less rapidly with altitude). However, the observed changes are small.

For what concerns the evolution of the controlled variables (peak heat flux and heat load), this is shown in Figure 10. The colour of the pericentre points changes from black to light grey when approaching the aerobraking end, thus giving the idea of which is the forced evolution of the controlled variables. The red upper boundary curve is clearly never trespassed.

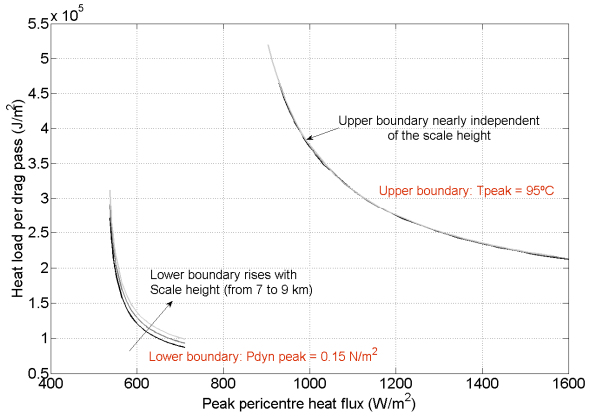

Figure 8: 2-D corridor sensibility to scale height assumption

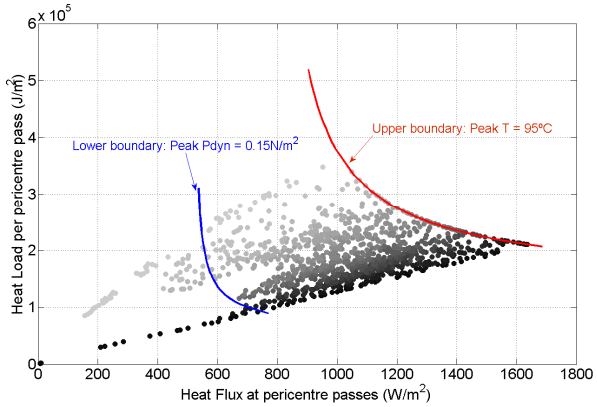

Figure 10: 2-D corridor simulation, Heat Flux and Heat Load evolution throughout aerobraking

For the following simulations, the corridors obtained with a scale height of 9 km have been used. At the aerobraking altitude (close to 100 km), typical scale heights are around 7 km for Mars and therefore, such assumption is conservative enough.

Figure 9 shows the pericentre altitude evolution and the effect of the aerobraking manoeuvres for a simulation performed with the 2-D corridor.

Figure 11 shows the pericentre heat flux as a function of the apocentre altitude for the 2-D corridor simulation. The highest pericentre heat flux values are up to 100 W/m^2 above the maximum allowed by the more conservative 1-D corridor.

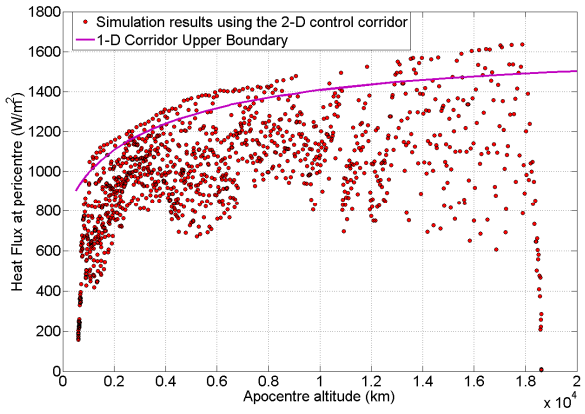

Figure 11: 2-D corridor simulation, Heat flux evolution Vs apocentre altitude

Figure 12 shows the altitude evolution for the aerobraking simulation performed with the 1-D control corridor. Clearly such evolution is very similar to what obtained with the 2-D corridor because the mission scenario is the same. However, the overall duration of the aerobraking is longer by approximately 15 days in the 1-D corridor simulation. The reason is clearly the non-optimality of the 1-D corridor method.

Figure 13 shows the evolution of the controlled variable (the peak heat flux) as a function of the apocentre altitude. The upper boundary curve is clearly never trespassed.

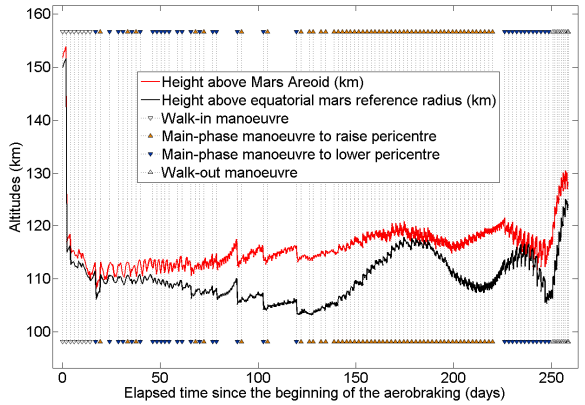

Figure 12: 1-D Corridor simulation, pericentre altitude evolution and ABMs effect

Figure 14 finally shows the evolution of the pericentre passes in the heat flux-heat load plane. Since the 1-D corridor approach is more conservative, the highest heat flux - heat load values are slightly lower than the upper boundary of the 2-D corridor.

Table 4 summarises the performance parameters of the aerobraking simulations obtained with the 1-D and 2-D corridor control. The 2-D corridor features an overall aerobraking duration about 15 days shorter and, at the same time, approximately 20 manoeuvres less. The overall cost of the aerobraking is similar in both cases, with a slight convenience of the 2-D corridor.

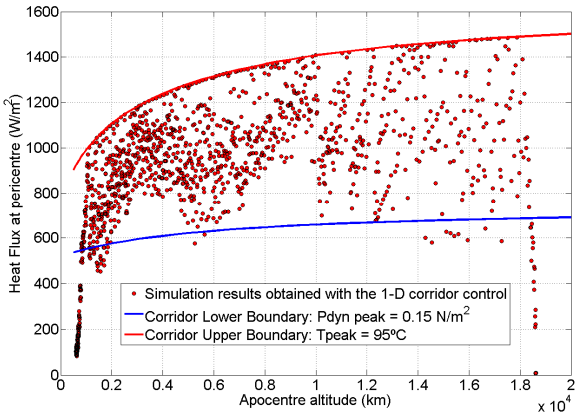

Figure 13: 1-D Corridor simulation, heat flux evolution Vs apocentre altitude

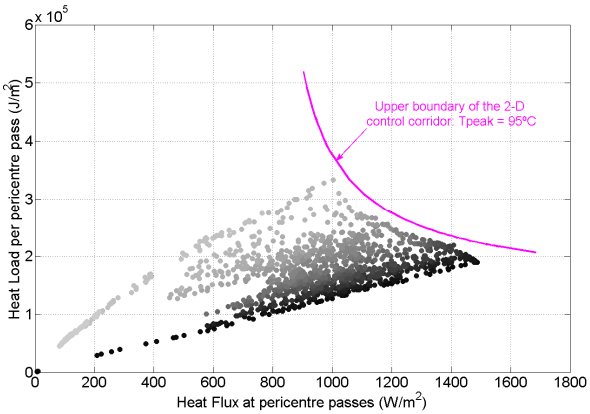

Figure 14: 1-D Corridor Simulation, Heat Flux and Heat Load evolution throughout the aerobraking

Table 4: MSRO Performance results with 1-D and 2-D corridor control

	1-D Corridor	2-D Corridor
Aerobraking duration (days)	**258.5**	**243.2**
Main Phase total cost (m/s)	20.6	19.5
Main Phase Nº of ABMs	84	68
Aerobraking total cost (m/s)	141.2	137.9
Aerobraking total Nº of ABMs	**101**	**80**

7. AEROBRAKING SIMULATION ON VENUS

In order to provide an example of an aerobraking about Venus, a "Magellan like" mission has been selected. The relevant aerobraking parameters are listed in Table 5. The aerobraking goal is to reduce the orbital period from an initial 3.2 hours down to 1.6 hours with a final pericentre of 200 km and a final apocentre of 540 km. The control interval for ABMs decisions is set to 2 days.

Table 5: AB parameters for simulation about Venus

Aerobraking parameters	Value
Initial orbital period (hours)	3.2
Initial inclination (deg)	45.0
Initial Walk-In pericentre altitude (km)	150.0
Number of Walk-In ABMs	3
Control interval duration (days)	2.0
Minimum allowed lifetime (days)	2.0
Reference altitude for lifetime computation (km)	300.0
Final orbit period (hours)	1.6
Final pericentre/apocentre altitude (km)	200 x 540
S/C ballistic coefficient (kg/m^2)	23.7

Orbit propagation takes into account the following:

- Sun gravity perturbation.
- Atmospheric drag modelled with the "Birkeland, Williams, Konopliv" model dating back to 1981

A 2-D control corridor has been defined using the parameters given in Table 6. A higher maximum allowable array temperature (130ºC) has been considered with respect to the MSRO scenario. This is because Venus atmosphere's uncertainty is much lower than Mars atmosphere's and hence the corridor can be defined with a lower temperature margin. The lower corridor boundary, on the other hand, has been computed again to assure a minimum peak dynamic pressure of 0.15 N/m^2.

The environment around Venus is characterised by a much greater solar flux and bond Albedo than around Mars. From a design point of view, this calls for the solar panels be more reflective than in the case of a Mars orbit in order to limit the array equilibrium temperature due to environment fluxes. For this reason a quite small absorption coefficient has been assumed: 25% versus the 90% used for the MSRO simulation. It is stressed that such values do not come from a detailed thermal analysis but have rather been assumed to produce a realistic aerobraking corridor.

Table 6: Solar array and environmental parameters for Venus AB corridor definition

Parameter	Value
Venus Bond Albedo	0.9
Solar array specific heat per unit surface (J/(K·m^2))	2241.0
Absorption coefficient of solar array back side coating, α_2	0.25
Absorption coefficient of solar cells, α_1	0.25
Emissivity coefficient of array back side, ε_2	0.79
Emissivity coefficient of solar cells, ε_1	0.87
Solar flux (W/m^2)	2611
Maximum allowable array temperature (ºC)	130
Minimum peak dynamic pressure (N/m^2)	0.15

Figure 15 shows the altitude evolution forced by the corridor control throughout the aerobraking. The overall duration is approximately 85 days and the pericentre altitude range is [135, 150] km.

Figure 16 shows the evolution of the control variables (peak heat flux and heat load) throughout the aerobraking. No violation of either the upper boundary or the lower boundary is observed during the Main Phase (during the Walk-Out phase control is based on lifetime).

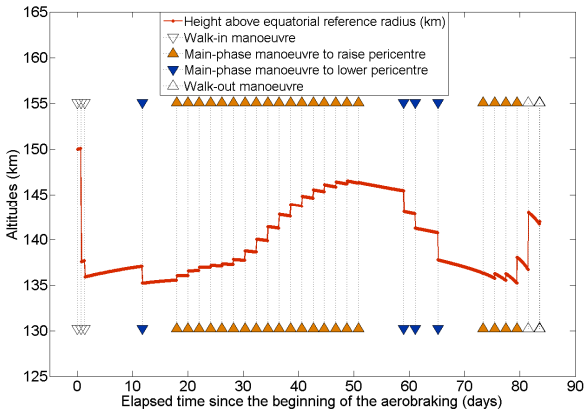

Figure 15: Altitude evolution and ABMs effect

Figure 17 shows the evolution of peak heat flux and dynamic pressure with time. During more than half of the aerobraking the natural trend of these control variables is to rise because the local solar time at pericentre approaches 3 pm, which is the hour of the day presenting the highest density at a given altitude (at least for the Venus atmospheric model used for the simulation). In the final part of the aerobraking, as the local solar time decreases, the pericentre density at a given altitude tends to decrease rapidly, thus requiring some pericentre lowering ABMs (see Figure 15).

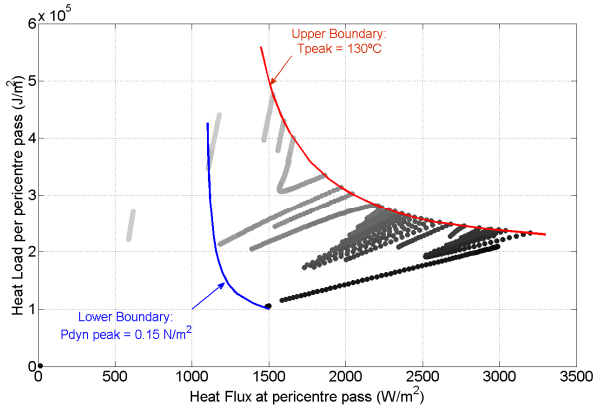

Figure 16: Control variables evolution throughout the aerobraking

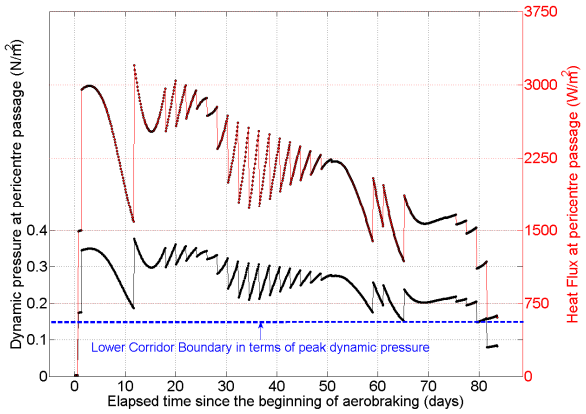

Figure 17: Peak heat flux and dynamic pressure evolution throughout the aerobraking

The dependence of the pericentre density on the LST is clearly shown in Figure 18. As this approaches 3 pm, the density rise urges that the pericentre altitude be raised up to more than 145 km.

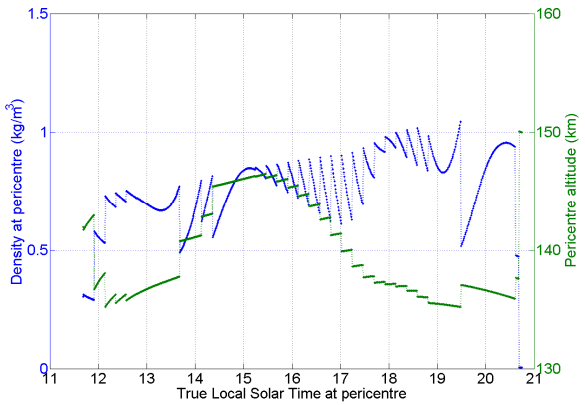

Figure 18: Pericentre altitude and density evolution as a function of the local solar time at pericentre

8. AEROBRAKING SIMULATION ON TITAN

The reference mission about Titan chosen for the simulation is the TSSM (Titan Saturn System Mission), scheduled for launch in 2020 and due to arrive 9 years later. The Titan segment of the mission envisages a detailed analysis of its atmosphere to be carried out while performing an aerobraking phase of 60 days. This duration is the minimum that must be ensured to permit the collection of sufficient science atmospheric data. The final orbit achieved will be a circular orbit of 1500 km altitude.

In order to aero-brake the S/C will use the High Gain Antenna and preliminary analysis showed that the peak heat flux ought to be maintained below 2500 W/m^2 [7]. No study of the drag duration effect on the maximum allowed peak heat flux is currently available.

The orbit achieved after the Titan Orbit insertion features 15000 km apocentre altitude and 720 km pericentre altitude. The very big effect of the Saturn's third body gravity effect translates into very large pericentre altitude variations of up to 50-100 km from orbit to orbit. Therefore a strict corridor control would be very expensive as it should counteract pericentre altitude variations of high frequency and magnitude.

This consideration, together with the fact that the actual goal is not to minimise the duration of the aerobraking but rather to perform it in two months, suggests to use an ad-hoc 1-D corridor control, shown in **Figure 19**. When the apocentre altitude maintains above 10000 km (and Saturn's third body perturbation has the greatest influence), the allowed corridor width is the highest possible. Then, in order to comply with the 60 days AB duration constraint (neither longer nor shorter), the upper boundary is progressively lowered with an ad-hoc profile.

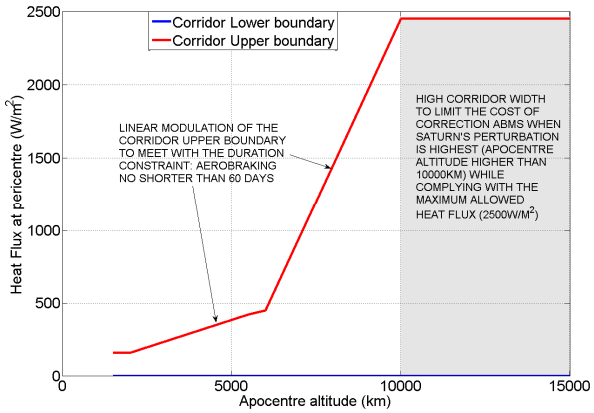

Figure 19: Ad-Hoc 1-D Corridor definition

The aerobraking parameters characterising the simulation are summarised in Table 7, whereas orbit propagation takes into account the following effects:

- Sun and Saturn gravity perturbation.
- Atmospheric drag modelled with the "Yelle" Titan atmosphere model

Table 7: AB parameters for simulation about Titan

Aerobraking parameters	Value
Initial orbital period (days)	0.82
Initial inclination (deg)	85.0
Initial Walk-In pericentre altitude (km)	680.0
Number of Walk-In ABMs	2
Control interval duration (days)	2.0
Minimum allowed lifetime (days)	4.0
Reference altitude for lifetime computation (km)	1000.0
Final circular orbit altitude (km)	1500.0
S/C ballistic coefficient (kg/m^2)	71.62

Figure 20 shows the evolution of the pericentre altitude and the effect of the control ABMs. All manoeuvres aim at raising the pericentre to either follow the corridor upper boundary modulation or to counteract the natural pericentre altitude drift. Finally a short Walk-Out phase maintains the lifetime above 4 days, while reaching the final orbit altitude of 1500 km. Figure 21 shows the evolution of the peak heat flux with the apocentre altitude.

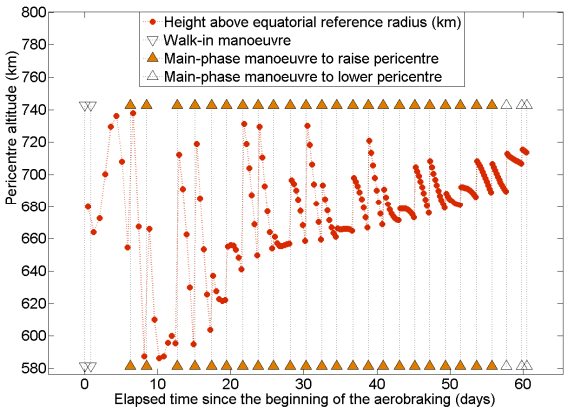

Figure 20: Altitude evolution and ABMs effect

Figure 22 shows the evolution of the peak heat flux and dynamic pressure at pericentre throughout the aerobraking, while Figure 23 shows the evolution of the orbital period. The highest variation is obtained at the beginning when the corridor width is highest.

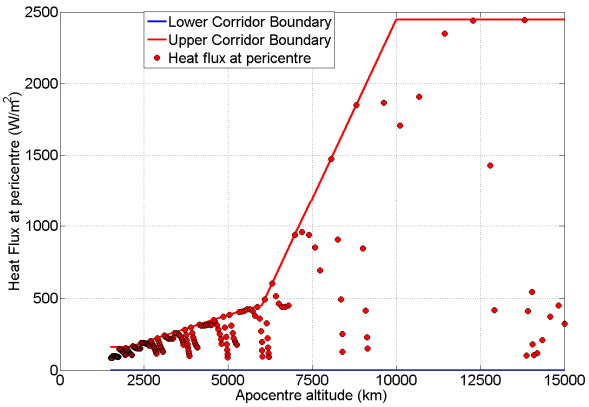

Figure 21: Heat Flux evolution Vs Apocentre altitude

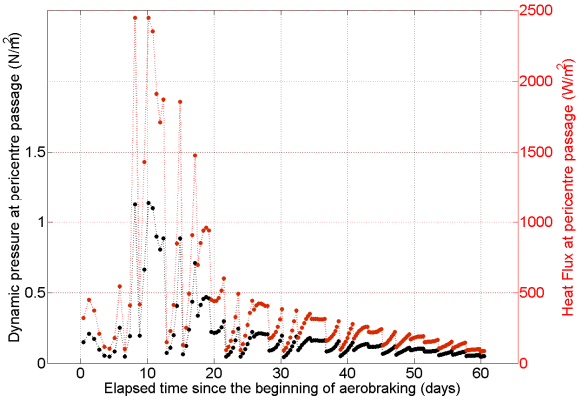

Figure 22: Heat Flux and dynamic pressure evolution with time

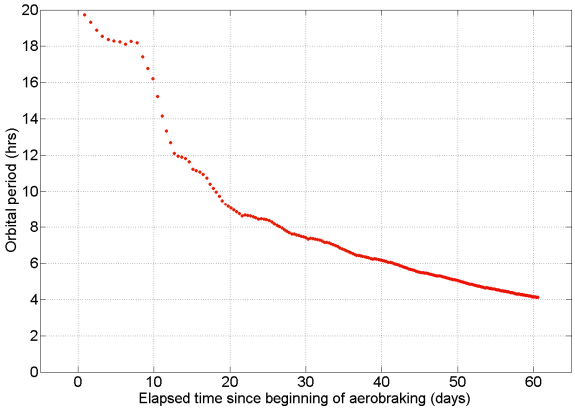

Figure 23: Orbital period evolution

9. CONCLUSIONS

Some innovative solutions of the aerobraking corridor control problem have been implemented.

First of all, a possible approach for the control ABMs computation has been proposed, that is based on:

- Selection of control surrogate variables: peak dynamic pressure or heat flux (for 1-D corridors), or peak heat flux and heat load (for 2-D corridors)
- Prediction of the control variables evolution throughout a selectable interval of time, named **control interval**. This represents also the fixed interval of time between successive ABM decisions throughout the aerobraking Main Phase.
- Computation of the control ABM size, if necessary, that enables the maximisation of the apocentre reduction while complying strictly with the corridor upper boundary

Secondly, two feasible solutions for the aerobraking corridor definition have been described and compared with the pure approach based on the solar array peak temperature. In order to define such corridors it has been necessary to:

- Define a simplified solar array thermal model, with the assumption of physical properties related to environment (planet radius, gravity and albedo), solar array (absorption and emissivity coefficients) and S/C (ballistic coefficient)
- Define an algorithm to compute the maximum permitted heat flux and heat load at a given apocentre altitude yielding to the maximum allowable solar array temperature. Expressing the maximum heat flux as a direct function of the apocentre altitude, a 1-D corridor has been defined, whereas, by expressing the maximum permitted heat flux as a function of the maximum permitted heat load, a 2-D corridor definition has been obtained.

Finally, the two corridor concepts have been tested with different scenarios around Mars, Venus and Titan. For Mars, a comparison between the 1-D and 2-D corridor concepts has been performed showing that the latter approach is a little more efficient.

An aerobraking simulation around Venus has been performed with a 2-D corridor control showing the applicability of this concept to a planet with an extremely different environment with respect to Mars.

On the other hand, an example of a 1-D corridor application has been provided for aerobraking around Titan. This simulation has shown that the 1-D corridor approach is adaptable to other types of aerobraking constraints different from peak solar array temperature. An ad-hoc definition of the 1-D corridor has permitted to limit the deltaV cost necessary to counteract Saturn's gravity perturbation and to achieve the aerobraking in the requested time (60 days).

The work presented in this paper has been carried out in the context of the activity "Robust and Autonomous Aerobraking Strategies" funded by the European Space Agency.

10. REFERENCES

1. F. Cichocki, S. Cornara, M. Sanchez, J.L. Cano, *Aerobraking Mission Analysis Tool for Mars Exploration Missions*, IPPW7 conference, June 2010

2. D.T. Lyons, J.G. Beerer, P. Esposito, M.D. Johnston, W.H. Willcockson, *Mars Global Surveyor: Aerobraking Mission Overview*, Journal of Spacecraft and Rockets, May-June 1999.

3. P. Esposito, V. Alwar, S. Demcak, E. Graat, M. Johnston and R. Mase., *Mars Global Surveyor Navigation and Aerobraking at Mars*, AAS 98-384.

4. J.C. Smith, J.L. Bell, *2001 Mars Odyssey Aerobraking*, AIAA 2002-4532.

5. S.M. Long, T.H. You, C.A. Halsell et al., *Mars Reconnaissance Orbiter Aerobraking Navigation Operation*, AIAA 2008-3349.

6. S.R. Lewis, M. Collins, P.L. Read, *A climate database for Mars*, Journal of Geophysical Research-Planets. 1999

7. D. T. Lyons, N. Strange, *Aerobraking at Titan*, AAS 09-358